Journal of Alloys and Compounds 480 (2009) 529–533

Contents lists available at ScienceDirect

Journal of Alloys and Compounds

journal homepage: www.elsevier.com/locate/jallcom

Nanocrystalline spherical iron–nickel (Fe–Ni) alloy particles prepared by ultrasonic spray pyrolysis and hydrogen reduction (USP-HR)

Sebahattin Gurmen[a,*], Burcak Ebin[a], Srećko Stopić[b], Bernd Friedrich[b]

[a] Istanbul Technical University, Metallurgical & Materials Engineering Department, Istanbul, Turkey
[b] IME Process Metallurgy and Metal Recycling, RWTH Aachen University, Aachen, Germany

ARTICLE INFO

Article history:
Received 19 November 2008
Received in revised form 19 January 2009
Accepted 22 January 2009
Available online 6 February 2009

Keywords:
Metals and alloys
Nanostructured materials

ABSTRACT

$FeCl_2$ and $NiCl_2$ were used for synthesis of nanocrystalline spherical Fe–Ni alloy particles by ultrasonic spray pyrolysis and hydrogen reduction (USP-HR). Spherical ultrafine Fe–Ni particles were obtained by USP of aqueous solutions of iron–nickel chloride followed by thermal decomposition of generated aerosols in hydrogen atmosphere. Particle sizes of the produced Fe–Ni particles can be controlled by the change of the concentration of an initial solution. The effect of the precursor solution in the range of 0.05, 0.1, 0.2 and 0.4 M on the morphology and crystallite size of the Fe–Ni alloy particles are investigated under the conditions of 1.5 h running time, 900 °C reduction temperature, and 1.0 L/min H_2 volumetric flow rate. X-ray diffraction (XRD) studies and Scherrer crystallite size calculations show that the crystalline size was nearly 28 nm. Energy dispersive spectroscopy (EDS) was performed to determine the chemical composition of the particles. Transmission electron microscope (TEM) was used to confirm the crystalline size, that was determined using XRD results. Scanning electron microscopy (SEM) observations reveal that the precursor solution strongly influences the particle size of the synthesized Fe–Ni alloy particles. Spherical nanocrystalline Fe–Ni alloy particles in the range of 80 and 878 nm were obtained at 900 °C.

1. Introduction

Nanoscale particle research has recently become a very important field in materials science. Such ultrafine metal powders often exhibit very interesting electronic, magnetic, optical, and chemical properties. Their unique features depend on particle size, shape, surface composition, and surface atomic arrangement [1–4]. Magnetic nanoparticles have important applications in catalysts, magnetic fluids, and high-density recording media. In such applications, composition of the particles is considered the key characteristic affecting their magnetic properties [5]. Although, many techniques have been developed to prepare ceramic and pure metallic nanoparticles, research on nanosized particles of metallic alloys is very few [6,7]. Methods that have been used to synthesis Fe–Ni alloy particles are mechanical alloying, the chemical method, spray pyrolysis, film deposition, levitation melting in liquid nitrogen and electrodeposition [7,8].

The spray pyrolysis method is applied to prepare spherical non-agglomerated submicron particles of complex composition and controlled phase content, suitable for direct application or fabrication of high technology sintered materials. Moreover, ultrasonic spray pyrolysis (USP) is a versatile technique for producing various materials in a wide range of composition, size and morphology [9,10]. USP of solutions is performed by applying a powerful source of ultrasound to the corresponding solution forming an aerosol with constant droplet size, which depends on the characteristic of the liquid and the frequency of the ultrasound. From the viewpoint of the application of the as-generated particles for advanced materials synthesis, particle morphology has great interest. It is presumed that certain particle morphology is formed during the evaporation/drying stage that encountered processes of evaporation and diffusion of both the solvent and solute, changing in droplet temperature and crust formation [9–11].

There is a lack of systematic studies to understand the possible production techniques of nanostructured Fe–Ni alloy particles. Ohno [12] has prepared particles made up of Fe–Ni alloys, which have been widely used as magnetic materials, by evaporating starting materials in an inert gas atmosphere at temperatures over 1600 °C. Li et al. [13] have focused on synthesis and properties of nanoparticles of Fe–Ni alloys in six compositions by hydrogen plasma reaction. The spherical Fe-Ni nanoparticles with a mean particle size less than 35 nm have been prepared. Dong et al. [14] have synthesized Fe–Ni nanoparticles ranging from 19 to 34 nm in their mean size using the hydrogen plasma reaction method in a mixture of H_2 and Ar. They have found that two phases with austenite and martensite structures coexist over a wide compositional range in the nanoparticles. The fabrication of nanocrystalline Fe–Ni alloy

* Corresponding author. Tel.: +90 212 285 68 62; fax: +90 212 285 34 27.
E-mail address: gurmen@itu.edu.tr (S. Gurmen).

0925-8388/$ – see front matter © 2009 Elsevier B.V. All rights reserved.
doi:10.1016/j.jallcom.2009.01.094

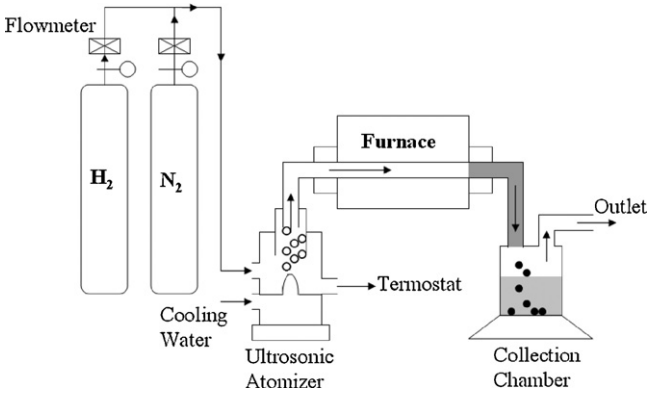

Fig. 1. Schematic drawing of experimental apparatus for the synthesis of nanocrystalline Fe–Ni particles.

particles by using ultrasonic spray pyrolysis and hydrogen reduction has not yet been investigated.

In this study, nanocrystalline Fe–Ni alloy particles were synthesized by ultrasonic spray pyrolysis and hydrogen reduction. The effects of the processing parameters on their size and crystalline structure were characterized by X-ray diffraction (XRD), transmission electron microscope (TEM), and scanning electron microscope (SEM).

2. Experimental

2.1. Materials

All the reagents ($FeCl_2{\cdot}4H_2O$ and $NiCl_2{\cdot}6H_2O$) were analytical grade and used without further purification. A water leach solution of $FeCl_2{\cdot}4H_2O$ and $NiCl_2{\cdot}6H_2O$ (powders were dissolved in deionized water for mixing of the salts) was used as starting material for this research. The deionized water (resistivity $\rho > 18\,M\Omega$) was used for all solutions. The concentration of the precursor solutions were between 0.05 and 0.4 M. All solutions were stirred for 1 h using a magnetic stirrer.

2.2. Experimental procedure

The nanocrystalline spherical Fe–Ni alloy particles were synthesized using the ultrasonic spray pyrolysis method. Fig. 1 shows the schematics of the apparatus. The experiments were done at 800 °C starting from iron–nickel chloride solution with concentrations of 0.05 and 0.4 M. Very fine droplets of the aerosol were obtained in an ultrasonic atomizer Pyrosol 7901 (Ramine Baghai Instrumentation, with a frequency of 2.1 MHz). The aerosol was transported by H_2-carrier/reduction gas via a quartz tube (0.7 m length and 0.02 m diameter) to an electrical heated furnace (Ströhlein, Germany) with a temperature control of ±1 °C. Because of the safety reasons and to create an inert atmosphere, nitrogen with a flow rate of 1.0 L/min was used prior to the reduction process. Under spray pyrolysis conditions in hydrogen atmosphere and at a flow rate of 1.0 L/min, the dynamic (continuous) reduction took place in the quartz tube reactor (heated zone 280 mm). The residence time, calculated from the ratio of the volume of the reaction zone and the carried gas flow, was about 5.3 s with the assumption that the rate of droplets and the carried gas are equal. X-ray diffractometer (Phillips PW 1700), SEM/energy dispersive spectroscopy (EDS) (Zeiss DSM 982 Gemini) and TEM (JEOL 2000 EX) were used for the characterization of the obtained Fe–Ni particles. For XRD analysis, the Fe–Ni dispersed particles were placed on a glass substrate and allowed to dry in air at room temperature. Crystalline structure and size was determined by XRD and TEM analysis. The chemical compositions of particles were investigated by EDS analyses. SEM images were used to observe the surface morphology of particles formed at different precursor solution. Particle size and size distribution were determined from SEM images by Leica Image Manager. All the clearly observed particles on the SEM images were taken into account in these analyses.

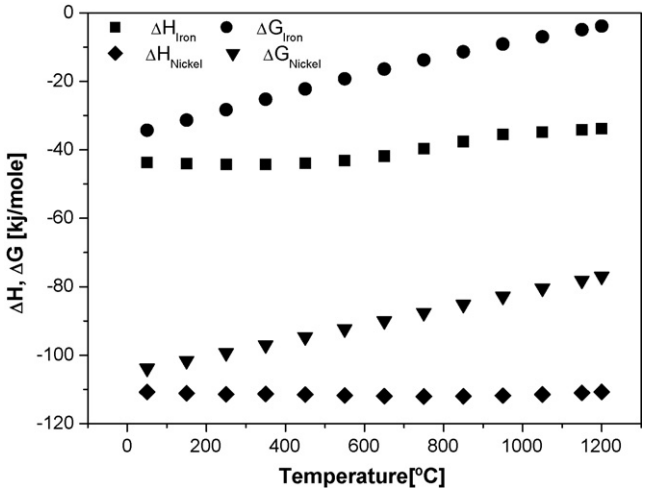

Fig. 2. Dependence of the Gibb's energy on the temperature.

The powders were first dispersed in ethanol and inserted in ultrasonic bath for 30 min. Then the suspension was dropped onto a grid for TEM analysis, and a glassy carbon slide to make a thick film, which later coated by palladium for SEM characterization.

Table 1 contains data for chemical composition of the applied solutions, conditions of the production process, and a short description of the obtained powders.

3. Results and discussion

3.1. Thermodynamic analysis of hydrogen reduction

The reaction for the formation of Fe–Ni metal from iron–nickel chloride can be described as in Eq. (1).

$$FeCl_2 + NiCl_2 + 2H_2 \rightarrow \text{Fe–Ni} + 4HCl \quad (1)$$

The thermodynamic analysis is done using FactSage Software and in the temperature range of 50 and 1200 °C (Fig. 2).

The values of Gibb's free energy (ΔG°) for the reaction (1) in the temperature range up to 1000 °C confirm the probability for formation of Fe–Ni from $FeCl_2 + NiCl_2$ by hydrogen reduction. Although Gibbs free energy is always negative between 0 and 1200 °C temperature range, it increases through the positive values at elevated temperatures.

Iron and nickel formation reactions from their chlorides are thermodynamically possible at desired reduction temperature, 900 °C. Thus, we supposed that the calculated residence time, 5.3 s, of the droplets/particles is sufficient for the transformation of droplets to metal particle in the hydrogen atmosphere according to model one particle from one droplet [15].

3.2. Structural analysis of Fe–Ni particles

Fig. 3 shows XRD patterns of the USP-HR Fe–Ni particles. The cubic crystalline Fe–Ni phase has three main peaks at the diffraction angles of 43.47°, 50.67° and 74.68°. In Fig. 3, a diffraction peak was observed at 43.7° and 50.9°. The broad hump at the low diffraction angles are coming from glass substrate which is amorphous. The X-

Table 1
Composition of precursor solutions, conditions of the process, and descriptions of the obtained powders ($T_{precursor}$ = 25 °C, test period = 1.5 h, volume of used solution = 340 ml).

No.	Concentration of precursor solution (M) ($FeCl_2{\cdot}4H_2O + NiCl_2{\cdot}6H_2O$)	Temperature (°C)	Flow rate of H_2 (L/min)	Characteristic of the product
1	0.05 M	900	1.0	Spherical, nanocrystalline Fe–Ni particles
2	0.1 M	900	1.0	Spherical, nanocrystalline Fe–Ni particles
3	0.2 M	900	1.0	Spherical, nanocrystalline Fe–Ni particles
4	0.4 M	900	1.0	Spherical, nanocrystalline Fe–Ni particles

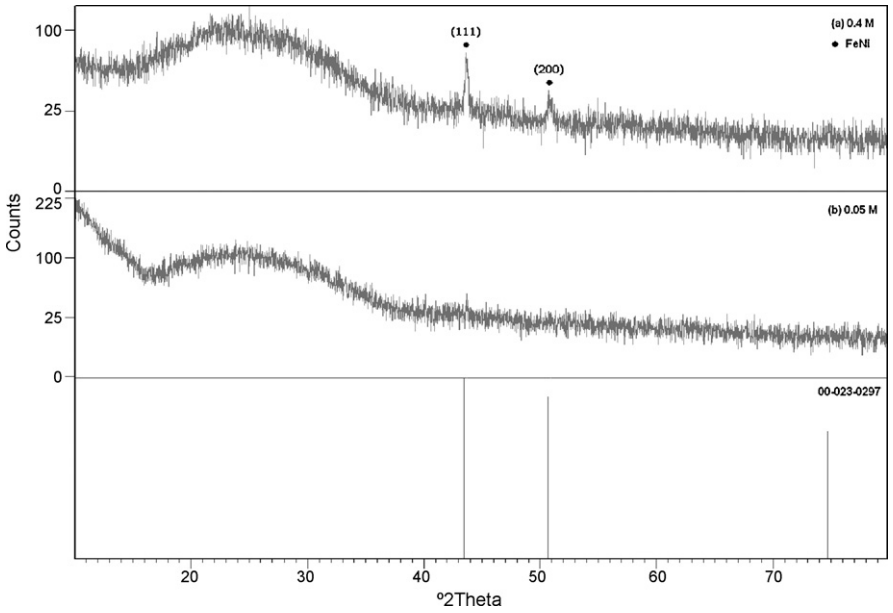

Fig. 3. X-ray analysis of the USP-HR Fe–Ni particles, (a) 0.4 M, 900 °C, 1.5 h, (b) 0.05 M, 900 °C, 1.5 h.

ray analysis of the powders indicated the presence of face centered cubic crystalline structured Fe–Ni nanoparticles and any diffraction peaks due to oxides phases of Fe–Ni were not observed.

Crystalline size calculated from XRD patterns by using Scherrer Equation,

$$t = \frac{K\lambda}{B\cos\theta} \quad (2)$$

defines a simple relationship between crystalline size, and peak width. In this equation, K is constant whose value is between 0.85, and 0.9, λ is the wavelength of the X-ray (Cu $K\alpha_1$ = 1.5418 Å), B is the full width high maximum, FWHM (in radians) of the peak due to size effect, θ is the Bragg angle, and t is the particle size. The (1 1 1) peak in Fig. 3a was used for the crystalline size determination by Scherrer formula. FWHM of the (1 1 1) peak is 0.32° at 43.7° and the calculated sizes of Fe–Ni crystallites for given parameters is 28 nm.

Although, the XRD results could give reliable knowledge about the crystalline size of the particles, direct information about particle structure can be obtained by TEM analysis. TEM bright field micrograph of the particles, prepared using 0.4 M precursor concentration, is displayed in Fig. 4. This image indicates that sizes of the crystallites were smaller than the 50 nm. So, it is obviously seen that TEM observation supported and confirmed the result of the XRD analysis.

3.3. The effect of precursor solution concentration

In this research the effect of the precursor concentration in the range of 0.05, 0.1, 0.2 and 0.4 M was investigated under the conditions of 1.5 h running time, 900 °C reduction temperature, and 1.0 L/min H_2 volumetric flow rate. Particle size, shape and morphology were indentified using SEM micrographs. SEM images of the obtained Fe–Ni particles are shown in Fig. 5.

The SEM images show the typical morphology of Fe–Ni alloy particles. The shape of the particles is nearly spherical with homogeneous size distribution. Fe–Ni particles in the range of 80–878 nm were prepared by using 0.4 M precursor concentration (see Fig. 5a). Large particles seen in Fig. 5a were formed by agglomeration of the smaller particles. On the other hand, decreasing the concentration in the precursor solution (from 0.4 to 0.2 M, and 0.1 and 0.05 M) reduced mean diameter of the particles, and increased the uniformity under the same reaction temperatures (see Fig. 5b and c). As it is seen from Fig. 5b average particle size is between 400 and 500 nm for 0.2 M concentration. Reducing of the solution concentration to 0.1 M cause the decreasing of average particle size between 250 and 350 nm. Agglomeration also took place on the large particles seen in Fig. 5c and d. Average size of Fe–Ni particles in Fig. 5d. was below 300 nm and the size distribution was more homogeneous. The smallest particle size was 80 nm under the 0.05 M precursor concentration (Fig. 5d and e). EDS results of Fe–Ni particles are shown in Fig. 6.

EDS results indicate that particles synthesized from all solution concentrations contain iron and nickel. Carbon peaks in the results exist due to substrate which is glassy carbon slide. Besides that, there is no impurity observed in the chemical composition of the particles caused by other reaction products such as chlorine.

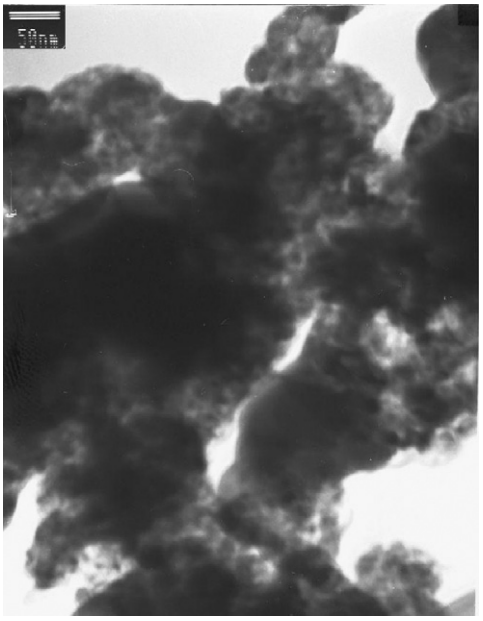

Fig. 4. TEM image of Fe–Ni particles obtained using 0.4 M precursor.

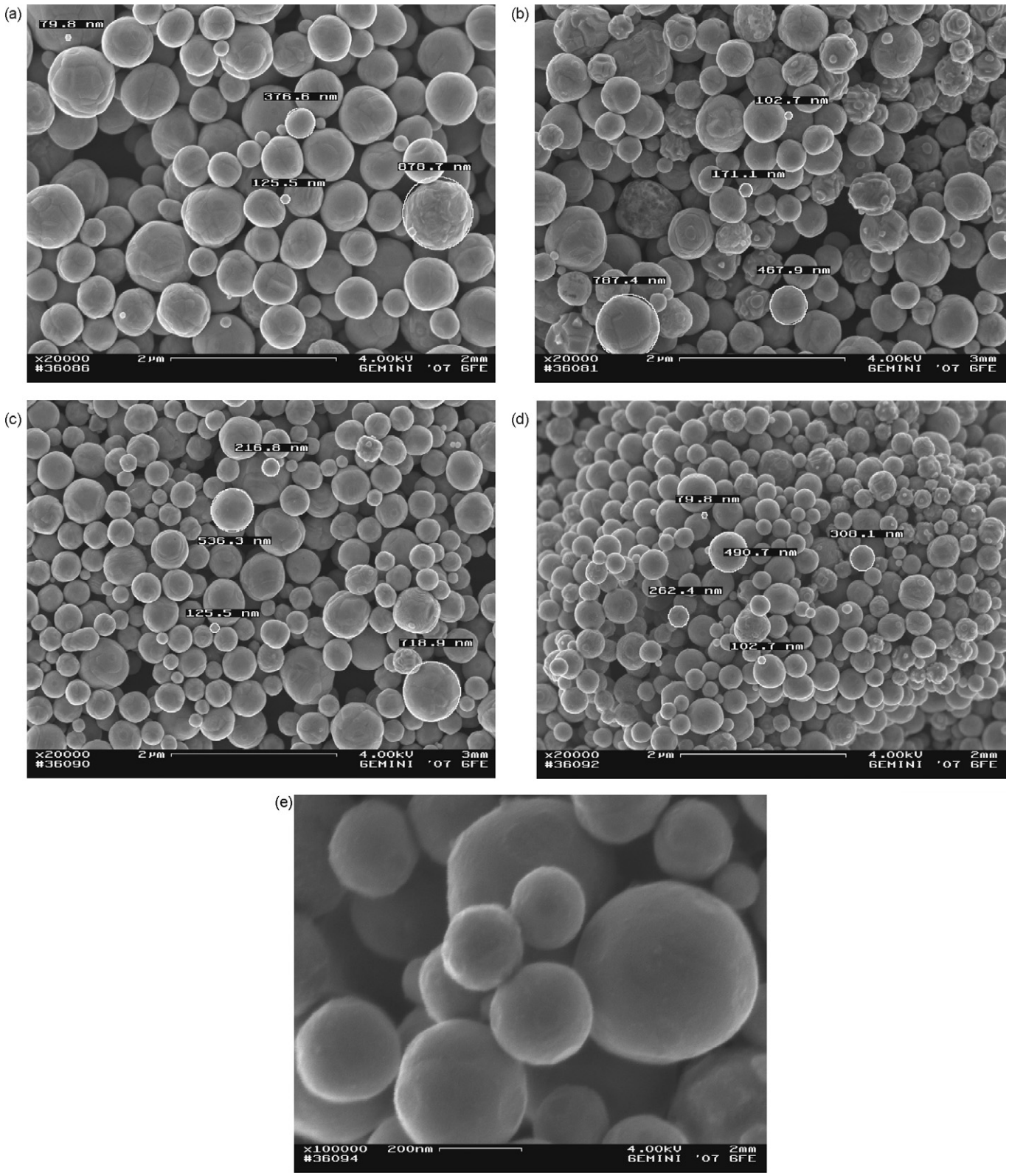

Fig. 5. SEM images of Fe–Ni particles prepared at 900 °C with different precursor concentration: (a) 0.4 M, (b) 0.2 M, (c) 0.1 M, (d) 0.05 M, and (e) higher magnification of (d) (0.05 M).

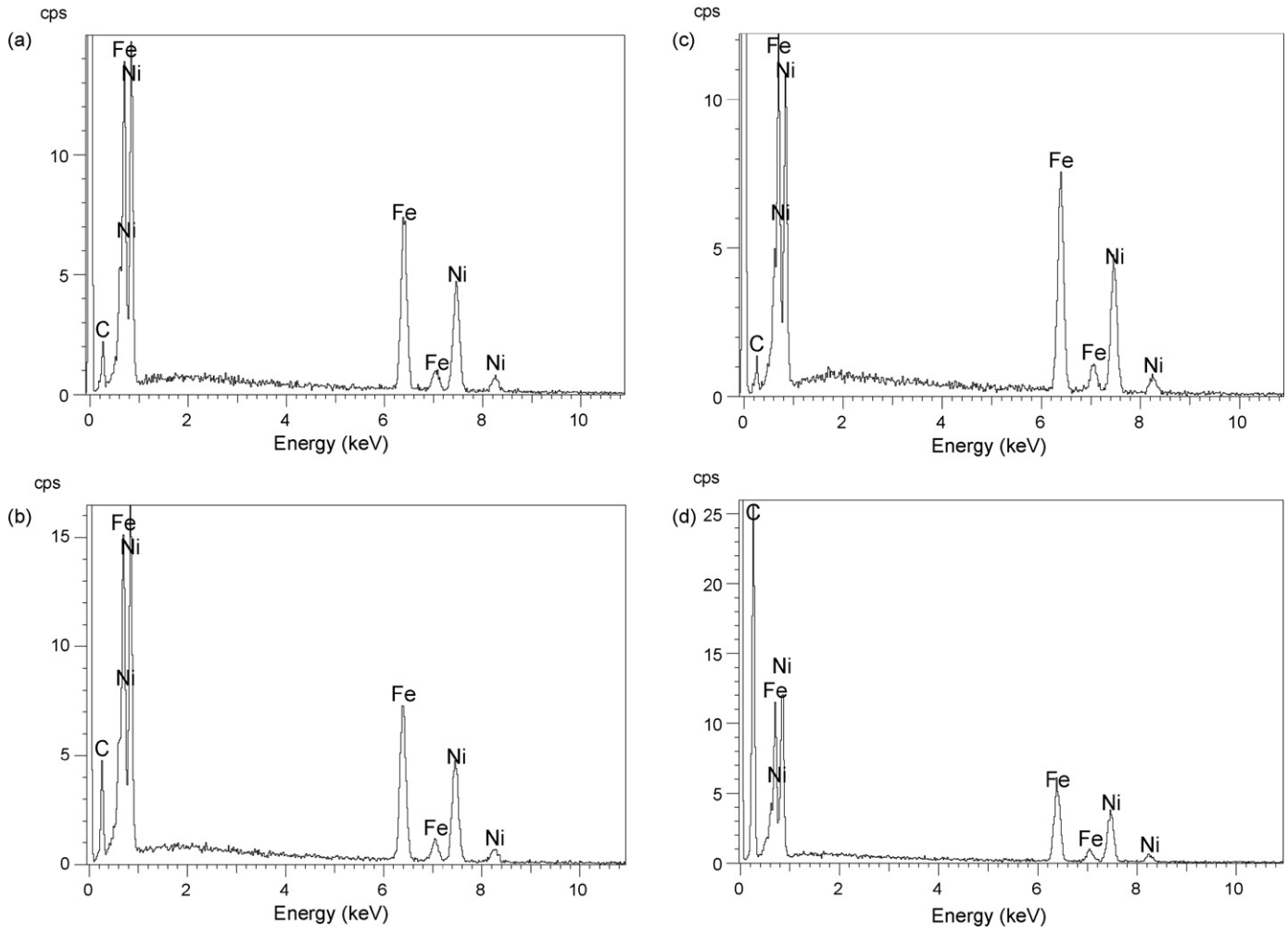

Fig. 6. EDS results of Fe–Ni particles obtained from (a) 0.4 M, (b) 0.2 M, (c) 0.1 M and (d) 0.05 M precursor concentrations.

4. Conclusion

As a result, ultrasonic spray pyrolysis was used for the synthesis of nanocrystalline spherical Fe–Ni particles from $FeCl_2{\cdot}4H_2O + NiCl_2{\cdot}6H_2O$ solution. The effect of the precursor solution in the range of 0.05, 0.1, 0.2 and 0.4 M on the morphology and crystallite size of the Fe–Ni alloy particles are investigated under the conditions of 1.5 h running time, 900 °C reduction temperature, and 1.0 L/min H_2 volumetric flow rate. The X-ray analysis of the particles indicated the presence of body centered cubic crystalline structured Fe–Ni nanoparticles. From XRD analysis, it is found that the crystallite size of the Fe–Ni alloy particle is 28 nm for 0.4 M precursor solution, and TEM image verified this result. The experimental results confirmed that reducing of the concentration of precursor solution decreases the mean particle size. In all cases, dense Fe–Ni particles show almost spherical morphology, homogeneous size distribution and smooth surface.

Acknowledgments

We would like to thank the Alexander von Humboldt Foundation for providing research fellowships to Dr. Sebahattin Gurmen allowing 2-month stay at the IME Process Metallurgy and Metal Recycling, RWTH Aachen University. Also we would like to thank Mr. Dieter Leimbach for his highly motivated assistance in our experimental part.

References

[1] A.I. Gusev, A.A. Rempel, Nanocrystalline Materials, Cambridge International Science Publishing, 2004.
[2] H. Duan, X. Lin, G. Liu, L. Xu, F. Li, J. Mater. Process. Technol. 208 (2008) 494–498.
[3] V. Jokanovic, Surfact. Sci. Ser. 130 (2006) 513–533.
[4] X.W. Wei, G.X. Zhu, J.H. Zhou, H.Q. Sun, Mater. Chem. Phys. 100 (2006) 481–485.
[5] Y.J. Suh, H.D. Jang, H. Chang, W.B. Kim, H.C. Kim, Powder Technol. 161 (2006) 196–201.
[6] X. Li, S. Takahashi, J. Magn. Magn. Mater. 214 (2000) 195–203.
[7] S.F. Moustafa, W.M. Daoush, J. Mater. Process. Technol. 181 (2007) 59–63.
[8] X.Y. Qin, J.S. Lee, J.G. Nam, B.S. Kim, Nanostruct. Mater. 11 (3) (1999) 383–397.
[9] S. Gürmen, S. Stopic, B. Friedrich, Mater. Res. Bull. 41 (2006) 1882–1890.
[10] K.K. Lee, Y.C. Kang, K.Y. Jung, J.H. Kim, J. Alloys Compd. 395 (2005) 280–285.
[11] J.H. Kim, V.I. Babushok, T.A. Germer, G.W. Mulholland, S.H. Ehrman, J. Mater. Res. 18 (2003) 1614–1622.
[12] T. Ohno, Jpn. J. Appl. Phys. 32 (1993) 4648–4651.
[13] X.G. Li, A. Chiba, S. Takahashi, J. Magn. Magn. Mater. 170 (1997) 339–345.
[14] X.L. Dong, Z.D. Zhang, X.G. Zhao, Y.C. Chung, S.R. Jin, W.M. Sun, J. Mater. Res. 14 (1999) 398–406.
[15] S.C. Tsai, Y.L. Song, C.S. Tsai, C.C. Yang, W.Y. Chiu, H.M. Lin, J. Mater. Sci. 39 (2004) 3647–3657.